Structural and functional insights into the regulation mechanism of CK2 by IP_6 and the intrinsically disordered protein Nopp140

Won-Kyu Lee[a], Sang Hyeon Son[a], Bong-Suk Jin[a], Jung-Hyun Na[a], Soo-Youl Kim[b], Kook-Han Kim[c], Eunice EunKyeong Kim[c], Yeon Gyu Yu[a,1], and Hyung Ho Lee[a,d,1]

Departments of [a]Bio and Nano Chemistry and [d]Integrative Biomedical Science and Engineering, Kookmin University, Seoul 136-702, Korea; [b]Cancer Cell and Molecular Biology Branch, Division of Cancer Biology, Research Institute, National Cancer Center, Goyang 410-769, Korea; and [c]Biomedical Research Institute, Korea Institute of Science and Technology, Seoul 136-791, Korea

Edited by John Kuriyan, University of California, Berkeley, CA, and approved October 15, 2013 (received for review March 21, 2013)

Protein kinase CK2 is a ubiquitous kinase that can phosphorylate hundreds of cellular proteins and plays important roles in cell growth and development. Deregulation of CK2 is related to a variety of human cancers, and CK2 is regarded as a suppressor of apoptosis; therefore, it is a target of anticancer therapy. Nucleolar phosphoprotein 140 (Nopp140), which is an intrinsically disordered protein, interacts with CK2 and inhibits the latter's catalytic activity in vitro. Interestingly, the catalytic activity of CK2 is recovered in the presence of D-*myo*-inositol 1,2,3,4,5,6-hexakisphosphate (IP_6). IP_6 is widely distributed in animal cells, but the molecular mechanisms that govern its cellular functions in animal cells have not been completely elucidated. In this study, the crystal structure of CK2 in complex with IP_6 showed that the lysine-rich cluster of CK2 plays an important role in binding to IP_6. The biochemical experiments revealed that a Nopp140 fragment (residues 568–596) and IP_6 competitively bind to the catalytic subunit of CK2 (CK2α), and phospho-Ser574 of Nopp140 significantly enhances its interaction with CK2α. Substitutions of K74E, K76E, and K77E in CK2α significantly reduced the interactions of CK2α with both IP_6 and the Nopp140-derived peptide. Our study gives an insight into the regulation of CK2. In particular, our work suggests that CK2 activity is inhibited by Nopp140 and reactivated by IP_6 by competitive binding at the substrate recognition site of CK2.

inositol hexakisphosphate | IDP | phosphorylation

Protein phosphorylation is a major aspect of signaling in cells including cell cycle (1). Casein kinase 2 (CK2) is a ubiquitous protein kinase that is essential for cell growth (2), development, and other essential cellular processes (3–7). More than 300 proteins that are involved in DNA replication, transcription, translation, and signal transduction are phosphorylated by CK2 (8). CK2 is also involved in the regulation of apoptosis (9, 10). CK2-dependent phosphorylation of AKT kinase, which is essential for cell survival, activates cells to resist apoptosis (11, 12). In addition, CK2-dependent phosphorylation of β-catenin, which induces cell proliferation by Wnt signaling, increases its stability and ability to resist proteolysis (13). Deregulation of CK2 is strongly related to a variety of human cancers (14–17), and therefore, CK2 is considered a target for anticancer therapy (18).

Structural and biochemical studies have revealed the molecular architecture and catalytic mechanism of CK2. CK2 consists of two catalytic subunits (α and α′) and two regulatory subunits (β) which can form $\alpha_2\beta_2$ or $\alpha\alpha'\beta_2$ heterotetramers (19). The crystal structure of the CK2 holoenzyme is composed of a central dimer of regulatory subunits with catalytic subunits bound to them (20). The active site and residues that are critical for substrate binding have been identified (21). The structure of CK2α in complex with an ATP-analog inhibitor showed a common ATP binding pocket that consists of the residues Lys68, Glu81, and Asp175 (22). Mutational analysis revealed that basic amino acids (74–77) are involved in substrate binding, which have negatively charged residues in the consensus recognition sequence (22). Despite the previous structural works, the regulatory mechanisms of CK2 still need to be determined. This is a difficult process as CK2 is a constitutive enzyme, and its activity is not affected by its phosphorylation, unlike other protein kinases involved in signal transduction pathways (23). In addition, CK2 is insensitive to typical second messengers such as cAMP, diacylglycerol, inositol 1,4,5-triphosphate (IP_3), and Ca^{2+} (24).

Inositol hexakisphosphate (IP_6) is naturally present in many plants (25). IP_6 is recognized as an important regulator of many cellular functions in animal cells, including signal transduction, cell proliferation, and differentiation (25). Recent study showed that CK2 mediates cell survival through phosphorylation of inositol hexakisphosphate kinase-2 by enhancing its ubiquitination (26). Previously, we have shown that nucleolar phosphoprotein 140 (Nopp140), which is a nucleolar protein, specifically binds to CK2α and inhibits its catalytic activity in vitro (27). It has also been shown that IP_6 prevents the interaction between CK2 and Nopp140, which is an intrinsically disordered protein (IDP) (27). The phosphorylated form of Nopp140 also binds the catalytic subunit of CK2α, and this interaction is interrupted by IP_6 (27). The application of the yeast two-hybrid method revealed that the interaction level between the C-terminal half of Nopp140 and the CK2α decreases when IP_6 is present. In other words, the IP_6 level drives the interaction level between the C-terminal half of Nopp140 and the CK2α inverse proportionally (28). Furthermore, adenomatous polyposis coli (APC) binds to CK2 and inhibits its activity (29). The binding site of APC to CK2 is constrained to the C-terminal region (29), which has sequence homology to Nopp140, thereby suggesting that Nopp140

Significance

Structural and functional studies on protein kinase CK2α, which is a ubiquitous kinase that can phosphorylate hundreds of cellular proteins, revealed that CK2α activity is inhibited by Nopp140 and reactivated by IP_6 by competitive binding at the substrate recognition site of CK2α. IP_6 binds to the lysine-rich cluster of CK2α, and phospho-Ser574 on Nopp140 significantly enhances its interaction with CK2α.

Author contributions: Y.G.Y. and H.H.L. designed research; W.-K.L., S.H.S., B.-S.J., J.-H.N., S.-Y.K., K.-H.K., and H.H.L. performed research; W.-K.L., E.E.K., Y.G.Y., and H.H.L. analyzed data; and W.-K.L., S.H.S., Y.G.Y., and H.H.L. wrote the paper.

The authors declare no conflict of interest.

This article is a PNAS Direct Submission.

Data deposition: The atomic coordinates and structure factors have been deposited in the Protein Data Bank, www.pdb.org (PDB ID code 3W8L).

[1]To whom correspondence may be addressed. E-mail: hhlee@kookmin.ac.kr or ygyu@kookmin.ac.kr.

This article contains supporting information online at www.pnas.org/lookup/suppl/doi:10.1073/pnas.1304670110/-/DCSupplemental.

and APC may have common binding motifs to CK2. However, the precise interaction site of Nopp140 to CK2α and the binding mode of CK2α and IP_6 have not been previously determined. Here, we determined the crystal structure of CK2α in complex with IP_6 using X-ray crystallography, and showed that IP_6 binds to the positively charged cluster, which accommodates the negatively charged residues of the substrate. We also determined that the residues 568–596 of Nopp140 are critical for its binding to CK2α, and phospho-Ser574 of Nopp140 significantly enhances its binding affinity to CK2α. Inhibition of CK2 activity by Nopp140, and the recovery of the suppressed CK2 activity by IP_6 suggest that IP_6 and the Nopp140 peptide competitively bind to a common motif of CK2.

Results

Amino Acids 568–596 and Phospho-Ser574 of Nopp140 Are Critical for Binding to CK2α. Previously, we have shown that the binding site of Nopp140 to CK2α is located at the C-terminal half of Nopp140 (28). To locate the precise binding region, we pursued a more detailed truncation analysis based on the estimations from sequence analyses (Fig. 1*A*). The presence of a C-terminal truncated Nopp140 variant (lacking residues 602–709) gradually reduced the specific interaction between Nopp140 and CK2α (Fig. 1*B*); however, the Nopp140 fragment containing residues 527–602 was able to bind to CK2α (Fig. 1 *A* and *D*). Phosphorylation of Nopp140 (527–602) significantly enhanced the binding affinity to CK2α, thereby suggesting that the phosphorylation contributes to its binding to CK2α (Fig. 1 *E* and *F*). IP_6 treatment of pNopp140 (1–709), Nopp140 (527–602), and pNopp140 (527–602) exhibited a diminished binding to CK2α, thereby suggesting that IP_6 competes with Nopp140 (527–602) for the same site on CK2α (Fig. 1 *C*–*E*).

To map the precise phosphorylation site on Nopp140, previously identified CK2 binding motifs were used to search Nopp140 based on sequence homology. As a result, three locations at 348–366 (P1, peptide 1), 454–472 (P2, peptide 2), and 576–596 (P3, peptide 3) showed potential sequence homology to the CK2 binding motifs (Fig. 2*A*). Synthetic peptides representing these three regions were tested for binding affinity to CK2α using a surface plasmon resonance (SPR) method. As shown in Fig. S1, P3 binds to CK2α more strongly than P1, and P2 fails to show any significant binding curve. The binding properties of both P1 and P3 suggest that at least two sites on Nopp140 are involved in CK2α binding with the P1 region possessing the highest binding affinity.

As Ser574 at N terminus of P3′ (extended peptide at N terminus of P3) is a potential phosphorylation site, the effect of phosphorylation at Ser574 was examined. Various peptides containing Ser574 or phospho-Ser574 were prepared (Fig. 2*A*), and their binding properties to CK2α were measured. As shown in Fig. 2*B*, the P3′ peptide including phospho-Ser574 showed the highest binding affinity, and the unphosphorylated form showed significantly reduced affinity (Fig. 2*B*). Likewise, shortened peptides containing Ser574 or phospho-Ser574 showed phosphorylation-dependent binding to CK2α (Fig. 2 *B*–*D*). These results indicate that the Nopp140 peptides containing the regions near Ser574 can bind CK2α, and the binding of Nopp140 is significantly enhanced by the phosphorylation of Ser574. Recently, structural disorder and local order of full-length Nopp140 was predicted based on various methods including ^{1}H NMR, differential scanning calorimetry, and protease sensitivity (30, 31), and the CK2α binding region (residues 527–602) of Nopp140 is also predicted to be disordered. The circular dichroism analysis of Nopp140 (527–602) revealed that the secondary structure mainly consists of random coils (Fig. S2). However, an α-helical structure was observed following the addition of trifluoroethanol.

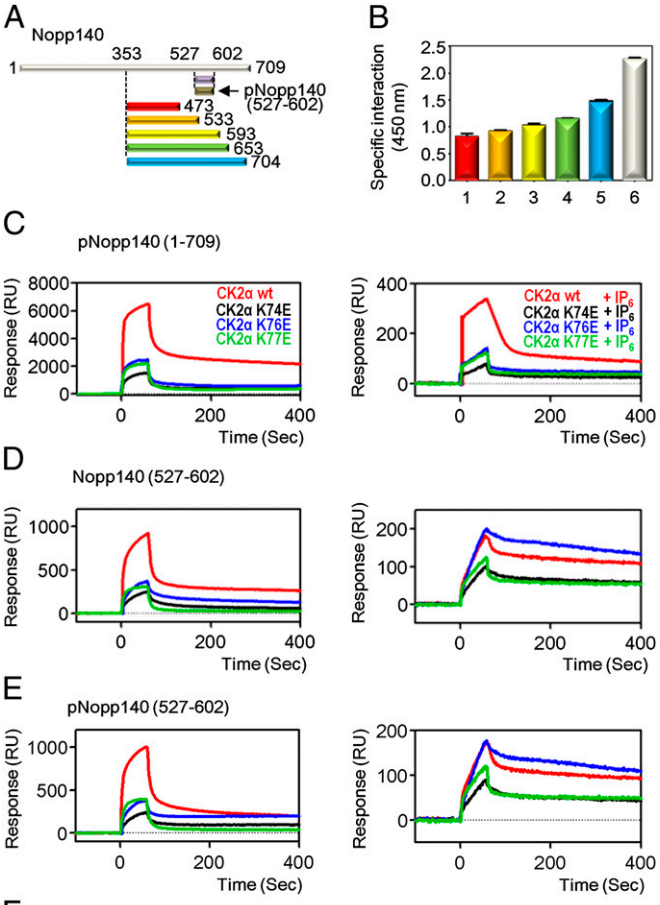

F

Nopp140 fragments	k_a ($M^{-1}s^{-1}$)	k_d (s^{-1})	K_D (nM)
Nopp140 (353-704)	9.5×10^5	1.1×10^{-3}	1.1
pNopp140 (353-704)	5.0×10^5	2.5×10^{-3}	5.0
Nopp140 (527-602)	1.0×10^5	1.3×10^{-2}	130
pNopp140 (527-602)	1.2×10^5	8.5×10^{-3}	72.5

Fig. 1. Mapping binding region of Nopp140 with CK2α and the inhibitory effect of IP_6. (*A*) Schematic representation of Nopp140 constructs. (*B*) Specific interaction between C-terminal domain of Nopp140 and CK2α observed using a modified ELISA method. Purified CK2α was immobilized on a plate, and the intensities of the chemiluminescence signal from the bound HRP-conjugated anti–His-tag antibody with His-Nopp140 fragments, 353–473 (red), 353–533 (orange), 353–593 (yellow), 353–653 (green), 353–704 (cyan), and 1–709 (white) were measured. (*C*) SPR sensorgrams of pNopp140 (1–709) with CK2α, CK2α wild type (colored in red), and CK2α mutants (K74E in black, K76E in blue, and K77E in green) were used as analytes with (*Right*) and without IP_6 (*Left*). (*D*) SPR sensorgrams of Nopp140 (527–602) with CK2α. The analytes were used as indicated in Fig. 1*C*. (*E*) SPR sensorgrams of pNopp140 (527–602) with CK2α. The analytes were used as indicated in Fig. 1*C*. (*F*) Kinetic data for the interaction between CK2α wild-type and Nopp140 fragments. Original SPR sensorgrams are shown in Fig. S3.

Crystal Structure of CK2α–IP_6 Complex. To gain further insight into the structural organization of the CK2α–IP_6 complex and its role in the stimulated activity of CK2 caused by blocking the interaction between Nopp140 and CK2α, we solved the crystal structure of CK2α in complex with IP_6. The crystal structure of the CK2α–IP_6 complex was determined at 2.4-Å resolution, and the refined model of the CK2α–IP_6 complex gave R_{work}/R_{free} values of 23.5/24.8% for 27.6- to 2.4-Å data (Table S1). The refined model accounts for residues 4–329 in each of the two monomers of CK2α in an asymmetric unit. The two monomers of CK2α in the asymmetric unit were almost identical to each other.

BIOCHEMISTRY

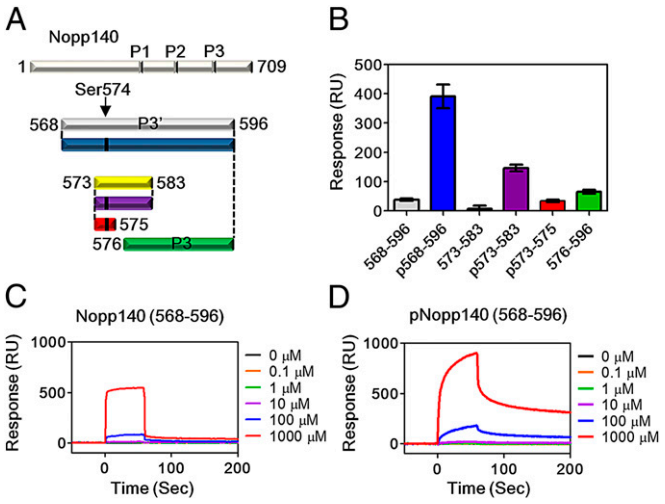

Fig. 2. Analysis of the narrow interaction region of Nopp140 and CK2α. (*A*) Schematic representation of full-length Nopp140, three Nopp140 peptides (P1, P2, and P3), and six P3′-derived peptides (colored in gray, blue, yellow, purple, red, and green). The position and phosphorylation of Ser574 is indicated by an arrow and black bar, respectively. (*B*) SPR analysis of the interaction between P3′-derived Nopp140 peptides and CK2α. Nopp140 (568–596), pNopp140 (568–596), Nopp140 (573–583), pNopp140 (573–583), Nopp140 (573–575), and Nopp140 (576–596) are represented by gray, blue, yellow, purple, red, and green columns, respectively. SPR sensorgrams of CK2α with (*C*) Nopp140 (568–596) and (*D*) pNopp140 (568–596) were obtained for 0.1, 1, 10, 100, and 1,000 μM Nopp140 peptides, respectively.

When monomer A was compared with the other monomer, the root-mean-square deviation averaged over the other monomer was 0.85 Å for 295 Cα atom pairs. The overall structure of CK2α shows the common bipartite architecture of protein kinases with a β-sheet–rich N-terminal domain and an α-helical C-terminal domain (Fig. 3*A*).

When the electrostatic potential was drawn, several positively charged patches were found on the surface of CK2α (Fig. 3*B*). Among them, conserved positively charged residues (Lys74, Lys76, Lys77, Arg80, and Lys83), along with semiconserved residues (Lys75 and Lys79), which form a lysine-rich cluster, were clustered on one side of CK2α (marked with a dotted circle in Fig. 3*B*). It is possible that one of these positively charged patches serves as the binding site of IP_6; however, there have been no experimental observations of biologically relevant IP_6 bound to CK2α. The crystal structure of the CK2α–IP_6 complex demonstrates that IP_6 binds to the cleft of CK2α between two domains (Fig. 3 *A*–*C*). It prompted us to check whether the IP_6 binding site is consistent with a substrate-binding site of CK2α. Until now, the crystal structure of CK2α in the presence of a substrate has not been solved (32), but it is known that substrates with acidic residues interact at positions P+1 and P+3 from the phosphorylation site (21). Two sulfate ions bind to the putative substrate-binding site of CK2α, which matches reasonably well with the acidic substrate sequence S/T-D/E-X-D/E (33). Given that the binding sites of sulfate ions in CK2α are also conserved among CMGC kinases, it is likely that these regions might be substrate-binding sites (34). Interestingly, one of the binding sites of sulfate ions on CK2α matches well with the IP_6 binding site (Fig. 3*A*), thereby suggesting that IP_6 and the substrates might share a common binding site. The reduced affinity of Nopp140 to CK2α in the presence of IP_6 also indicates that Nopp140 and IP_6 might share a common binding site on CK2α. These findings further support our proposed model that IP_6 competes with Nopp140 for CK2 binding. It appears that IP_6 binding to CK2α allows the substrate to access both the active site and substrate-binding site.

Lysine-Rich Cluster of CK2α Is Critical for Binding to Both IP_6 and Nopp140. In the structure of the CK2α–IP_6 complex, IP_6 molecules are clearly defined by their electron density (Fig. S4) and are bound near the active sites of the two chains of CK2α in the asymmetrical unit. Lys74 forms a direct hydrogen bond with the O24 atom of IP_6 (2.9 Å), whereas Lys76, Lys77, and Arg155 are positioned close to IP_6 without a direct hydrogen bond (Fig. 3*C*). Two phosphates of IP_6 form hydrogen bonds with nitrogen atoms of Arg191 (3.1 and 2.6 Å), whereas the nitrogen atom of Asn189 also makes hydrogen bonds with the O31 and O36 atoms of IP_6 (3.2 and 3.1 Å, respectively; Fig. 3*C*). All of the IP_6 binding residues (Lys74, Lys76, Lys77, Arg80, Arg155, Asn189, and Arg191) are strictly conserved among the CK2α homologs. To test whether the IP_6 binding site observed in the crystal structure of the CK2α–IP_6 complex is crucial for the interaction with IP_6 in solution, several lysines of CK2α (Lys74, Lys76, and Lys77) were substituted with Glu, and their interactions with IP_6 were examined using isothermal titration calorimetry (ITC). Indeed, the binding signals of the K74E, K76E, and K77E mutants of CK2α were significantly reduced compared with the signal of wild-type CK2α (Fig. 3*D* and Fig. S5), thereby indicating that the binding site of IP_6 is not a crystallographic artifact. Furthermore, the Lys74–Lys77 region of CK2α is critical for substrate binding, thereby suggesting that the binding of IP_6 at this site may contribute to the accessibility of substrate proteins by releasing Nopp140.

The structure shows that one of the phosphate groups of IP_6 is not recognized by CK2α (Fig. 3*C*); however, our previous study showed that D-*myo*-inositol 1,2,3,4,5-pentakisphosphate (IP_5), which lacks one phosphate at the C6 carbon of IP_6, is not nearly as potent as IP_6 in reactivating CK2α in the presence of Nopp140 (27). To explain this in light of the structure, we exactly defined the stereochemistry of IP_6 bound to CK2α, which fits well with the experimental electron-density map (Fig. S4), based on the

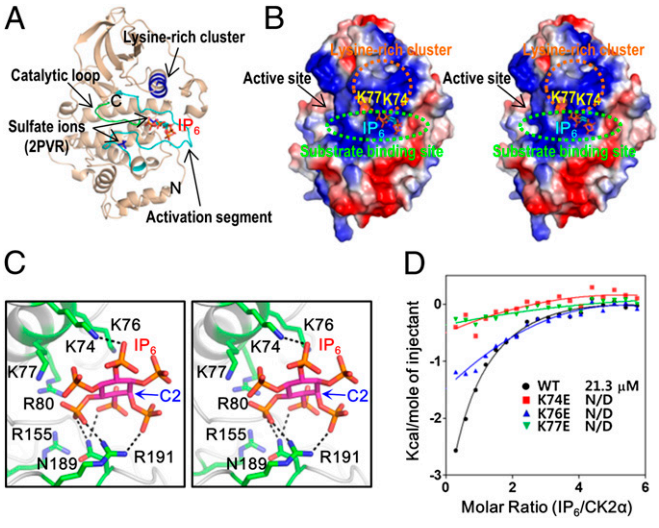

Fig. 3. Crystal structure of CK2α in complex with IP_6. (*A*) Ribbon diagram of the CK2α–IP_6 complex. The positions of the activation segment, catalytic loop, and lysine-rich cluster are indicated. Sulfate ions are incorporated from the structure of CK2α in complex with sulfate ions (PDB ID code 2PVR). (*B*) Stereoview of the electrostatic potential at the molecular surface of CK2α. IP_6 is represented by a stick diagram. (*C*) A close-up stereoview of IP_6 binding to CK2α. The black dotted lines denote hydrogen bonds. (*D*) ITC of IP_6 into CK2α solution. The wild-type CK2α and its mutants (K74E, K76E, and K77E) were titrated against IP_6. Original ITC data are shown in Fig. S5. N/D denotes the dissociation constant (K_D) is not determined.

rule that the phosphate at C2 carbon exists for vertical orientation, whereas the other phosphates at C1, C3, C4, C5, and C6 carbons exist for horizontal orientations (Fig. S4). When we checked the position of the phosphate of IP_6 at C6 carbon, which is missing in IP_5, the additional phosphate at C6 carbon is crucial for binding to CK2α, as it is positioned close to Lys74 and Lys77, facilitating the formation of hydrogen bonds (Fig. 3*C*). Hence, IP_6 binds more tightly to CK2α than does IP_5. D-*myo*-Inositol 1,2,4,5,6-pentakisphosphate missing phosphate at C3 position of IP_6 might work similar to the IP_6 because the phosphate at C3 does not contribute to the binding of IP_6 to CK2α (Fig. 3*C*).

Conformations of Plastic Regions of CK2α–IP_6 Complex. Functionally crucial plastic segments of CK2α include the glycine-rich loop, helix αC, β4/β5 loop, interdomain hinge region, catalytic loop, activation segment, and helix αI (Fig. 4*A*). The conformations of the plastic segments are controlled by CK2α regulators, including the noncatalytic subunit CK2β. CK2β can induce the active conformation of CK2α from the diverse conformations, and quickly shifts CK2α to a fully active state (35). In another study, the inactive state of CK2α was also found when glycerol bound to the remote cavity of CK2α, which resulted in a closed interdomain hinge region and a collapsed glycine-rich loop (35). In the structure of the CK2α–IP_6 complex, the IP_6 molecule bound to CK2α near the activation segment away from the active site (Fig. 3*A*). We also examined the structural changes in the plastic segments to check whether IP_6 binding to CK2α affected the conformation (Fig. 4*A*). When distance plots between the CK2α–IP_6 complex and the corresponding Cα positions of several CK2α structures (PDB ID codes 2PVR, 3H30, and 3JUH) containing various conformations of the plastic segments were drawn as a function of residue number, the differences between the CK2α–IP_6 complex and other CK2α structures were found to be significant (3~5 Å) with respect to the glycine-rich loop, helix αC, β4/β5 loop, interdomain hinge region, and helix αI (Fig. 4*A*). The CK2α–IP_6 complex adopts an open state of the interdomain hinge region and a stretched glycine-rich loop (Fig. 4*B*), thereby suggesting that the CK2α–IP_6 complex is catalytically active as active CK2α adopts an open state of the interdomain hinge region and a stretched glycine-rich loop (36).

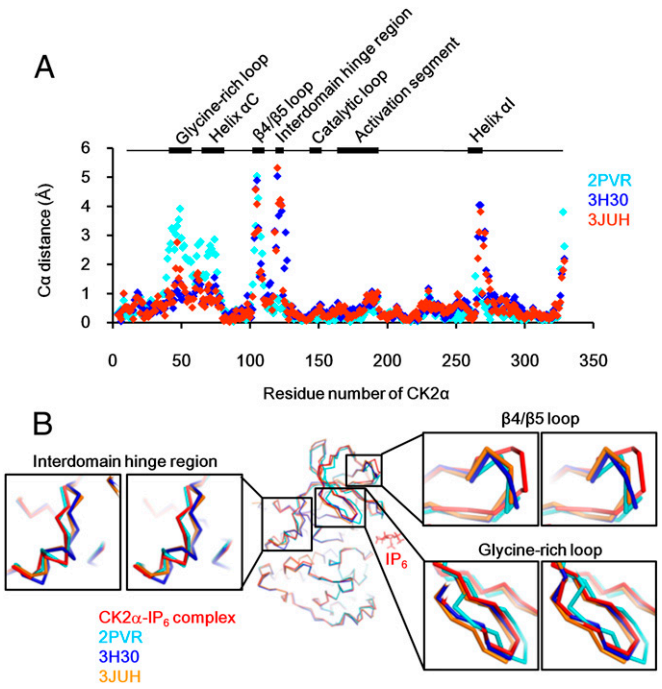

Fig. 4. Conformations of variable regions of CK2α. (*A*) Distance plots between the Cα position of the CK2α–IP_6 complex and the corresponding Cα positions of various CK2α structures (PDB ID codes 2PVR, 3H30, and 3JUH colored in cyan, blue, and orange, respectively). The rectangles above the plots represent the positions of variable regions of CK2α. (*B*) Stereoview of superposition of the CK2α–IP_6 complex (red) with various CK2α structures (PDB ID codes 2PVR, 3H30, and 3JUH colored in cyan, blue, and orange, respectively).

Overexpression of Nopp140 Suppresses Cellular Phosphorylation Activity of CK2. Previous studies have shown that Nopp140 binds to CK2α and inhibits CK2-dependent phosphorylation of α-casein and PCTP in vitro (27); however, the in vivo inhibitory effect of Nopp140 on CK2 has not been reported yet. In this study, we examined the effect of Nopp140 on the cellular activity of CK2 using α-casein as a substrate. In HeLa cells, the expression of Nopp140 was significantly increased when they were transfected with a Nopp140 expression vector (pNopp) and reduced to undetectable levels in the presence of siRNAs targeting Nopp140 (siNopp) (Fig. 5*A*). The phosphorylation of α-casein in the presence of the lysate from cells transfected with pNopp140 decreased to 75% (Fig. 5*B*, second bar), compared with phosphorylation in the presence of the lysate from the untreated cells. However, knockout of Nopp140 hardly affected the catalytic activity of CK2 (Fig. 5*B*, third bar). In contrast, treatment with 5,6-dichloro-1-(β-D-ribofuranosyl) benzimidazole (DRB), which is a specific inhibitor of CK2, reduced the catalytic activity of CK2 to 60% (Fig. 5*B*, fourth bar). A significant amount of α-casein was phosphorylated in the DRB-treated cell lysates, thereby suggesting that more than one-half of the α-casein could be phosphorylated by DRB-independent cellular kinases. These observations indicate that overexpression of Nopp140 suppresses more than one-half of the cellular activity of CK2 considering that the DRB-dependent phosphorylation is responsible for the CK2-dependent phosphorylation of α-casein.

To analyze the effect of Nopp140 on the phosphorylation of a variety of cellular proteins, phosphoproteins in HeLa cells treated with pNopp or siNopp were examined using an anti-phosphoserine antibody. The levels of certain phosphoproteins from cells overexpressing Nopp140 were significantly different to the untreated cells (Fig. 5*C*). For example, the phosphorylations in the 20- to 35-kDa range (Fig. 5*C*, lane 2, arrowheads) were significantly reduced in cells overexpressing Nopp140; however, this range was hardly effected by the Nopp140 knockdown (Fig. 5*C*, lane 3). The phosphorylations of marked proteins were decreased by DRB (Fig. 5*C*, lane 4), thereby indicating that they are substrates of CK2. These results showed that overexpression of Nopp140 can prevent CK2-dependent phosphorylation of certain CK2 substrates.

Model of CK2α Regulation by IP_6 and Nopp140. The characterizations of the CK2α–IP_6 structure, identification of a more precise binding site of Nopp140 to CK2α, and the competitive binding of Nopp140 and IP_6 to the common site on CK2α demonstrated in this study enable a possible model of CK2α regulation by IP_6 and Nopp140 to be proposed (Fig. 6). A free state of CK2 (holoenzyme or catalytic subunit) is fully active and phosphorylates its target proteins including Nopp140. Once Ser574 of Nopp140 is phosphorylated, it tightly binds to the substrate-binding site of CK2α and inhibits CK2α by blocking the access of other CK2 substrates, which have lower affinities than the phosphorylated form of Nopp140. When the level of Nopp140 is reduced or the concentration of IP_6 is increased to 20–40 μM, CK2α can dissociate from Nopp140 and become active. Substrate proteins that have higher affinity to CK2 than IP_6 might be phosphorylated by CK2 when the levels of IP_6 are decreased to the background level. It should be noted that high concentrations of IP_6 may interfere with the binding of substrates and inhibit CK2 because it blocks the binding of substrate

BIOCHEMISTRY

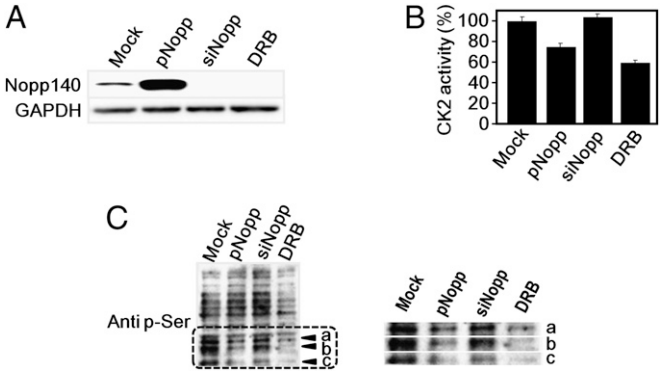

Fig. 5. In vivo inhibitory effect of Nopp140 on CK2. (*A*) Overexpression or knockdown of Nopp140. HeLa cells were transfected with the Nopp140 expression vector (pNopp) or siRNAs targeting Nopp140 (siNopp). For the Western blot, 20 μg of the proteins from the cleared lysates were used. (*B*) Negatively regulated CK2 activity by Nopp140. The cleared lysates of the HeLa cells transfected with pNopp or siNopp were incubated with α-casein. The reaction was further reacted with Kinase-Glo, and the luminescence intensity was measured using a microplate luminometer. The CK2 inhibitor DRB was used as a reference under the same conditions. All experiments were performed in triplicate. (*C*) Selectively regulated CK2 activity by Nopp140. The lysates of the HeLa cells treated with DRB or transfected with pNopp140 or siNopp140 were immunoblotted with phosphoserine antibodies.

proteins. Indeed, high concentrations of IP_6 slightly reduce the activity of CK2, probably by reducing the accessibility of the substrate proteins to CK2α. Because hundreds of proteins are proposed to be phosphorylated by CK2α, the substrates of CK2 probably have a wide range of affinities to CK2. Therefore, the phosphorylation of the substrate proteins of CK2 that has lower affinities to CK2 than Nopp140 but higher affinities than IP_6 would be affected by Nopp140 and IP_6.

Discussion

A regulatory role for IP_6 in cellular processes in animal cells has been proposed due to the presence of 10–30 μM IP_6 in animal cells and the involvement of IP_3, which is the precursor of IP_6 synthesis, in signal transduction; however, molecular details regarding the effects of IP_6 on cellular signals are yet to be elucidated. In this study, the crystal structure of CK2α in complex with IP_6, and binding analysis of CK2α mutants with IP_6 demonstrate that the clustered positively charged residues interact with the phosphate groups of IP_6 and indicate that charge–charge interactions contribute to the specific interaction between CK2α and IP_6 (Fig. 3*C*). The binding site of Nopp140 on CK2α is localized to residues 568–596, and the phosphorylation at Ser574 significantly enhances the affinity to CK2α. The sequence around Ser574 of Nopp140 contains a consensus CK2-recognition site, and therefore, after phosphorylation, phospho-Ser574 could serve as a CK2 recognition site. The negatively charged residues

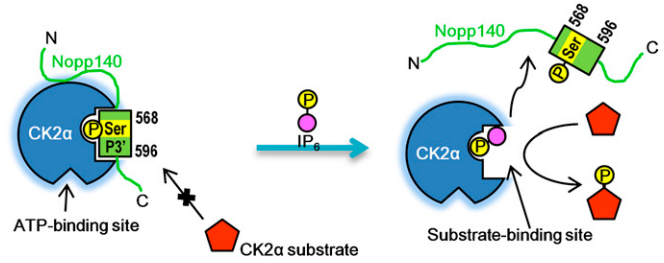

Fig. 6. Proposed model of CK2α regulation by IP_6 and Nopp140.

of the consensus sequence (Ser/Thr-X-X-Glu/Asp) and the phosphate group of phospho-Ser574 are thought to bind to the clustered region of CK2α where IP_6 binds (33).

The identification of CK2 inhibitory proteins such as Nopp140 and the highly phosphorylated metabolite IP_6 imply a novel regulation system for this protein. Unlike secondary signaling molecules such as cAMP, Ca^{2+}, and IP_3, Nopp140 is located in a confined region, the nucleolus, and interacts with several proteins. Therefore, tight association of CK2 with Nopp140 could define the repressed state of CK2 at specific confined regions of cells and/or provide CK2 substrates by delivering the target proteins to CK2 by interaction with other regions of Nopp140. More than 90% of the 700-aa-long protein Nopp140, which includes a CK2 binding region, consists of disordered structures. IDPs like Nopp140 mainly function by interaction with other proteins. Specifically, a long stretch of the IDP often engages in the interaction with multiple proteins. Furthermore, IDPs can contact multiple sites of their target proteins (37). These multiple interactions were also observed in the interaction between Nopp140 and CK2. At least two regions of Nopp140 in the C terminus half were shown to be involved in the interaction with CK2 (Fig. 2), where Ser574 largely contributes to the strongest binding property of Nopp140 to CK2. It should also be noted that Nopp140 demonstrates sequence homology with the C terminus of APC, which is a component of the β-catenin, GSK, and axin complex (29). The C-terminal region of APC is disordered and inhibits CK2 activity. The inhibitory activity of CK2 by Nopp140 and APC, especially via their disordered regions, suggests a more general regulatory function of IDPs to protein kinases. In vivo inhibitory activity of Nopp140 on CK2 suggests that Nopp140 could be exploited as a negative regulator of CK2. Furthermore, preliminary cell biological works involving the overexpression of Nopp140 suggest possible roles of Nopp140 in the β-catenin signaling pathway and TRAIL-mediated apoptosis as described in *SI Text* (Figs. S6 and S7).

The crystal structure of CK2α in complex with IP_6, together with the binding studies of Nopp140 and CK2α, and the Nopp140-dependant regulation of CK2 in vivo provide insight into the regulation of CK2 by IP_6 and Nopp140. We propose that Nopp140 is a negative regulator of CK2 and the activity of CK2 is reactivated by IP_6 by competitive binding at the substrate recognition site of CK2. This finding sheds light on the previously unknown regulatory mechanisms of CK2 by IP_6 and Nopp140.

Materials and Methods

Crystallization and Data Collection. Crystals of CK2α were grown by the sitting-drop vapor diffusion method at 296 K by mixing equal volumes (1 μL each) of the protein solutions (14.1 mg/mL) and the reservoir solutions. Before crystallization, the CK2α protein was mixed with IP_6 (Merck) at 1:30 molar ratio. A reservoir solution consisting of 17% (wt/vol) polyethylene glycol 4000, 15% (vol/vol) glycerol, 8.5% (vol/vol) isopropanol, and 0.085 M sodium Hepes (pH 7.5) was used to grow the crystals of CK2α. The crystals of CK2α grew to approximate dimensions of 0.07 × 0.07 × 0.3 mm within a few days. The crystals of the CK2α–IP_6 complex were frozen using a cryoprotectant solution containing 25% (wt/vol) polyethylene glycol 4000 in the crystallization mother liquor. X-ray diffraction data were collected at 100 K using an ADSC Quantum 270 CCD detector system (Area Detector Systems Corporation) at the experimental station BL-7A of the Pohang Light Source, Korea. For each image, the crystal was rotated by 1°. The raw data were processed and scaled using the HKL2000 program suite (38). Table S1 summarizes the statistics of data collection. The CK2α–IP_6 complex crystal belongs to the space group $P2_1$, with unit cell parameters of a = 70.14 Å, b = 56.57 Å, c = 95.54 Å, and β = 96.14° (Table S1). Two monomers of CK2α are present in the asymmetric unit, thereby giving a crystal volume per protein mass (V_M) of 2.36 $Å^3 \cdot Da^{-1}$ and a solvent content of 48% (vol/vol).

Structure Determination and Refinement. A cross-rotational search followed by a translational search was performed using the Phaser program (39). Subsequent manual model building was performed using the COOT program (40) and restrained refinement was performed using the REFMAC5

program (41). Several rounds of model building, simulated annealing, positional refinement, and individual *B*-factor refinement were performed. Table S1 lists the refinement statistics.

Measurement of the Interaction Between Nopp140 and CK2 and SPR Analysis. The interaction between Nopp140 and CK2α was examined by measuring the amount of phosphorylated Nopp140 that was bound to the immobilized GST-CK2α using HRP-labeled His-tag antibodies as previously described (28). SPR analysis of the interaction between Nopp140 and CK2α was performed using ProteOn XPR36 system (Bio-Rad). Nopp140 or CK2α were immobilized on the ProteOn HTG or GLH sensor chip (Bio-Rad) following the protocol described in the instruction manual, respectively. Sensorgrams for all of the binding interactions were recorded in real time and analyzed after subtracting the data from the control channel. After each measurement, the surface of the sensor chip was regenerated using 300 mM EDTA or 0.5 M NaCl, respectively. The dissociation and rate constants were calculated using the ProteOn Manager (Bio-Rad).

ACKNOWLEDGMENTS. We thank the staff at Beamline 7A of the Pohang Light Source for their assistance during the X-ray experiments and Dr. R. M. Gengan (Durban University of Technology) for valuable discussions. This work was supported by National Research Foundation of Korea Grants 2010-0021725, 2010-359-C00022, 2012K1A3A1A09033383, and 2013R1A1A1008195, and Korea Carbon Capture and Sequestration Research and Development Center Grant 2013M1A8A1038187.

1. Lee HH, Elia N, Ghirlando R, Lippincott-Schwartz J, Hurley JH (2008) Midbody targeting of the ESCRT machinery by a noncanonical coiled coil in CEP55. *Science* 322(5901):576–580.
2. Tawfic S, et al. (2001) Protein kinase CK2 signal in neoplasia. *Histol Histopathol* 16(2): 573–582.
3. Seldin DC, Leder P (1995) Casein kinase II alpha transgene-induced murine lymphoma: Relation to theileriosis in cattle. *Science* 267(5199):894–897.
4. Ahmed K, et al. (2000) Significance of protein kinase CK2 nuclear signaling in neoplasia. *J Cell Biochem Suppl* 35(Suppl 35):130–135.
5. St-Denis NA, Litchfield DW (2009) Protein kinase CK2 in health and disease: From birth to death: The role of protein kinase CK2 in the regulation of cell proliferation and survival. *Cell Mol Life Sci* 66(11-12):1817–1829.
6. Lebrin F, Chambaz EM, Bianchini L (2001) A role for protein kinase CK2 in cell proliferation: Evidence using a kinase-inactive mutant of CK2 catalytic subunit alpha. *Oncogene* 20(16):2010–2022.
7. Li D, et al. (1999) Expression of the casein kinase 2 subunits in Chinese hamster ovary and 3T3 L1 cells provides information on the role of the enzyme in cell proliferation and the cell cycle. *J Biol Chem* 274(46):32988–32996.
8. Meggio F, Pinna LA (2003) One-thousand-and-one substrates of protein kinase CK2? *FASEB J* 17(3):349–368.
9. Duncan JS, et al. (2010) Regulation of cell proliferation and survival: Convergence of protein kinases and caspases. *Biochim Biophys Acta* 1804(3):505–510.
10. Ahmad KA, Wang G, Unger G, Slaton J, Ahmed K (2008) Protein kinase CK2—a key suppressor of apoptosis. *Adv Enzyme Regul* 48:179–187.
11. Di Maira G, et al. (2005) Protein kinase CK2 phosphorylates and upregulates Akt/PKB. *Cell Death Differ* 12(6):668–677.
12. Guerra B (2006) Protein kinase CK2 subunits are positive regulators of AKT kinase. *Int J Oncol* 28(3):685–693.
13. Song DH, et al. (2003) CK2 phosphorylation of the armadillo repeat region of beta-catenin potentiates Wnt signaling. *J Biol Chem* 278(26):24018–24025.
14. Stalter G, et al. (1994) Asymmetric expression of protein kinase CK2 subunits in human kidney tumors. *Biochem Biophys Res Commun* 202(1):141–147.
15. Daya-Makin M, et al. (1994) Activation of a tumor-associated protein kinase (p40TAK) and casein kinase 2 in human squamous cell carcinomas and adenocarcinomas of the lung. *Cancer Res* 54(8):2262–2268.
16. Faust RA, Tawfic S, Davis AT, Bubash LA, Ahmed K (2000) Antisense oligonucleotides against protein kinase CK2-alpha inhibit growth of squamous cell carcinoma of the head and neck in vitro. *Head Neck* 22(4):341–346.
17. Yenice S, et al. (1994) Nuclear casein kinase 2 (CK-2) activity in human normal, benign hyperplastic, and cancerous prostate. *Prostate* 24(1):11–16.
18. Sarno S, et al. (2002) Toward the rational design of protein kinase casein kinase-2 inhibitors. *Pharmacol Ther* 93(2-3):159–168.
19. Gietz RD, Graham KC, Litchfield DW (1995) Interactions between the subunits of casein kinase II. *J Biol Chem* 270(22):13017–13021.
20. Niefind K, Guerra B, Ermakowa I, Issinger OG (2001) Crystal structure of human protein kinase CK2: Insights into basic properties of the CK2 holoenzyme. *EMBO J* 20(19):5320–5331.
21. Sarno S, et al. (1997) Mutational analysis of residues implicated in the interaction between protein kinase CK2 and peptide substrates. *Biochemistry* 36(39): 11717–11724.
22. Battistutta R, et al. (2007) The ATP-binding site of protein kinase CK2 holds a positive electrostatic area and conserved water molecules. *ChemBioChem* 8(15):1804–1809.
23. Guerra B, Issinger OG (1999) Protein kinase CK2 and its role in cellular proliferation, development and pathology. *Electrophoresis* 20(2):391–408.
24. Li D, Meier UT, Dobrowolska G, Krebs EG (1997) Specific interaction between casein kinase 2 and the nucleolar protein Nopp140. *J Biol Chem* 272(6):3773–3779.
25. Vucenik I, Shamsuddin AM (2006) Protection against cancer by dietary IP6 and inositol. *Nutr Cancer* 55(2):109–125.
26. Chakraborty A, et al. (2011) Casein kinase-2 mediates cell survival through phosphorylation and degradation of inositol hexakisphosphate kinase-2. *Proc Natl Acad Sci USA* 108(6):2205–2209.
27. Kim Y-K, Lee KJ, Jeon H, Yu YG (2006) Protein kinase CK2 is inhibited by human nucleolar phosphoprotein p140 in an inositol hexakisphosphate-dependent manner. *J Biol Chem* 281(48):36752–36757.
28. Lee W-K, et al. (2008) Characterization of the $InsP_6$-dependent interaction between CK2 and Nopp140. *Biochem Biophys Res Commun* 376(2):439–444.
29. Homma MK, Li D, Krebs EG, Yuasa Y, Homma Y (2002) Association and regulation of casein kinase 2 activity by adenomatous polyposis coli protein. *Proc Natl Acad Sci USA* 99(9):5959–5964.
30. Lee W-K, et al. (2012) Mitoxantrone binds to Nopp140, an intrinsically unstructured protein, and modulate its interaction with protein kinase CK2. *Bull Korean Chem Soc* 33(6):2005–2011.
31. Tantos A, et al. (2013) Structural disorder and local order of hNopp140. *Biochim Biophys Acta* 1834(1):342–350.
32. Niefind K, Raaf J, Issinger OG (2009) Protein kinase CK2 in health and disease: Protein kinase CK2: From structures to insights. *Cell Mol Life Sci* 66(11-12):1800–1816.
33. Meggio F, Marin O, Pinna LA (1994) Substrate specificity of protein kinase CK2. *Cell Mol Biol Res* 40(5-6):401–409.
34. Niefind K, Yde CW, Ermakova I, Issinger OG (2007) Evolved to be active: Sulfate ions define substrate recognition sites of CK2alpha and emphasise its exceptional role within the CMGC family of eukaryotic protein kinases. *J Mol Biol* 370(3):427–438.
35. Raaf J, Issinger OG, Niefind K (2009) First inactive conformation of CK2 alpha, the catalytic subunit of protein kinase CK2. *J Mol Biol* 386(5):1212–1221.
36. Niefind K, Issinger OG (2010) Conformational plasticity of the catalytic subunit of protein kinase CK2 and its consequences for regulation and drug design. *Biochim Biophys Acta* 1804(3):484–492.
37. Aoki K, Taketo MM (2007) Adenomatous polyposis coli (APC): A multi-functional tumor suppressor gene. *J Cell Sci* 120(Pt 19):3327–3335.
38. Otwinowski Z, Minor W (1997) Processing of X-ray diffraction data collected in oscillation mode. *Methods Enzymol* 276:307–326.
39. McCoy AJ, Grosse-Kunstleve RW, Storoni LC, Read RJ (2005) Likelihood-enhanced fast translation functions. *Acta Crystallogr D Biol Crystallogr* 61(Pt 4):458–464.
40. Emsley P, Cowtan K (2004) Coot: Model-building tools for molecular graphics. *Acta Crystallogr D Biol Crystallogr* 60(Pt 12 Pt 1):2126–2132.
41. Murshudov GN, Vagin AA, Dodson EJ (1997) Refinement of macromolecular structures by the maximum-likelihood method. *Acta Crystallogr D Biol Crystallogr* 53(Pt 3): 240–255.